

Supporting Information

Green light active photocatalyst for complete oxidation of organic molecules

Yue Yang,^a Akira Yamaguchi,^a Haoyang Jiang,^{a,b} Annabel van der Kooy,^c Sayuri Okunaka,^{d,e} Mariko Hosogai,^c Hiromasa Tokudome,^{e,*} and Masahiro Miyauchi^{a,*}

- a. Department of Materials Science and Engineering, Tokyo Institute of Technology
- b. College of Engineering and Applied Science, Nanjing University
- c. Department of Materials, University of Oxford
- d. Global Zero Emission Research Center (GZR), National Institute of Advanced Industrial Science and Technology (AIST)
- e. Research Institute, TOTO Ltd.

Note 1

Preparation of Fe(III)-BiVO₄ catalyst

Bismuth oxide, vanadium oxide, iron (III) chloride hexahydrate, sodium hydroxide, and titanium(IV) chloride were purchased from Wako Co., Ltd.

1. Preparation of BiVO₄

Bismuth vanadate was synthesized by a solid-state reaction between Bi₂O₃ and V₂O₅. A stoichiometric mixture of the two reactants was ground by a planetary ball milling machine at 200 rpm for 2 h. Ethanol was added as a milling medium. The ball milled chemicals were collected and then calcined in a muffle furnace for 5 h with the temperature increasing by 5°C per minute until 600°C was reached, from which point onwards the temperature was kept constant. Subsequently, the chemicals were thoroughly ground then further calcined at 800 °C for 2 h. The final product was then ground once more.

2. Preparation of Fe(III) grafted BiVO₄

Fe (III) was modified through an impregnation method. Specifically, 20 mL water, 1g of BiVO₄ and a set amount of FeCl₃ (corresponding to the desired Fe(III) loading wt%) were combined and the mixture was stirred at 400 rpm for 1 h on a hot plate set at 90 °C. The suspension was then filtered using a 0.025 μm (Millipore) membrane filter and dried at 80 °C for over 12 h. In this research, we varied the Fe(III) loading amount from 0.4 wt% to 0.8 wt% in steps of 0.1 wt% to determine the optimum amount for visible light photocatalytic activity.

3. Preparation of Ti(IV)-Fe(III) co-grafted BiVO₄

To further improve photocatalytic activity, we grafted Ti(IV) nanoclusters, which act as oxidation promoters,^{1,2} in addition to Fe(III)nanoclusters. The Ti(IV) modification was done using the same impregnation method as previously reported.¹ TiCl₄ was used as the Ti(IV) source. BiVO₄ powder, water, and TiCl₄ were combined and then the mixture was stirred for 1 h on a hot plate set at 90 °C before being filtered through a 0.025 μm (Millipore) membrane filter. Finally, it was dried at 80 °C for over 12 h. Fe(III) modification was subsequently performed using the procedure outlined in 2.

4. Preparation of Fe(III) grafted BiVO₄ treated with Alkaline solution

As another means to improve activity, we treated BiVO₄ powder with alkaline solution before grafting on Fe(III).³ BiVO₄ powder was soaked in 10 mL of 3 wt% aqueous NaOH solution. This mixture was stirred for 1 h on a hot plate set as 90 °C and then filtered through a 0.025 μm (Millipore) membrane filter. Finally, it was dried at 80 °C for over 12 h. Fe(III) modification was subsequently performed using the procedure outlined in 2.

Note 2

Characterization

XRD patterns were measured over a 2θ range of 3- 90° by a Rigaku SmartLab diffractometer with a D/teX Ultra detector. TEM and STEM images, and EDS (Energy-dispersive X-ray spectroscopy) mapping were taken by a JEOL JEM-2010F TEM. The UV-Vis spectra were recorded by a JASCO V-670 spectrometer using an integration sphere unit (diffuse reflectance method) in the 300-800 nm wavelength range with BaSO₄ used for baseline calibration. The Hard X-ray Photoelectron Spectroscopy (HXPES) was measured at Spring-8 beamline BL15XU. Electron spin resonance (ESR) was analyzed by a Bruker ESR Nano in a nitrogen atmosphere at the liquid nitrogen temperature either under light irradiation or in dark conditions. Ionization potential of powder photocatalyst was characterized by a photoemission yield spectroscopy (PYS), AC-3, RIKEN KEIKI. Photoluminescence (PL) spectra were evaluated by Fluorescence Spectrophotometer F-7000, HITACHI.

Note 3

Determination of bandgap

The bandgap of BiVO₄ was calculated using a Tauc plot with $h\nu$ as the x-axis and $(\alpha h\nu)^{1/r}$ as the y axis, where h , ν and α are the Planck constant, the frequency of light, and the Kubelka-Munk value obtained from UV-Vis spectra, respectively.

The value of r is related to the bandgap of the semiconductor: for direct bandgap semiconductors, r is 1/2, while for indirect bandgap semiconductors, r is 2. According to previous research, BiVO₄ is a direct bandgap semiconductor,⁴ so we use $r = 1/2$.

Note 4

Details about flat band potential evaluation by Mott-Schottky plot

1. Preparation of the BiVO₄ electrode.

A paste of BiVO₄ was made by mixing BiVO₄ powder, α -terpineol (Kanto Chemical Co., Inc.), and ethyl cellulose (Sigma Aldrich Corp.) together. This paste was then screen printed on an FTO substrate for 1 cycle and annealed at 450 °C for 2 h.

2. Preparation of the Fe(III)-BiVO₄ electrode.

Fe(III) was grafted onto BiVO₄ electrode through a similar impregnation method as described in Supporting Information, Note 1. Prepared BiVO₄ electrode was soaked into 50 mL 0.0018 M FeCl₃·6H₂O solution. This solution was then been kept stirred at 200 rpm for 1 h on a hot plate which is set as 90 °C.

3. Flat band potential evaluation by Mott-Schottky plot

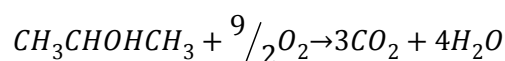
The flat band potential was evaluated by a Mott-Schottky plot using a three-electrode system with BiVO₄, Ag/AgCl, and Pt as the working electrode, reference electrode, and counter electrode, respectively. 0.5 M Na₂SO₄ was used for the electrolyte. All potentials (vs Ag/AgCl) can be converted to RHE using the following equation $E_{\text{RHE}} = E_{\text{AgCl}} + 0.0591 \cdot \text{pH} + 0.199 \text{ V}$

Note 5

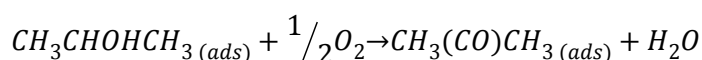
Supposed decomposition pathway of photocatalysis

1. Decomposition pathway of IPA

IPA decomposition pathway was well discussed by Arsac's work^{5,6}. The overall reaction of gaseous IPA is



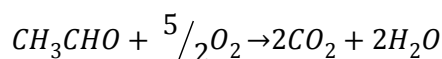
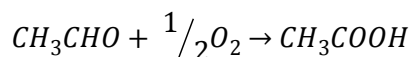
Acetone is the single route for the photocatalytic oxidation of IPA to CO₂ and H₂O⁶.



A kinetic model is proposed in their research which indicates that the competitive chemisorption between reactant IPA and product acetone is the key process of photocatalytic oxidation of IPA. More competitive chemisorption of acetone is favorable for complete oxidation of IPA. As compared to the conversion from IPA to acetone, reaction rate for conversion of acetone to CO₂ is lower since it includes a multi-hole involved process.

2. Decomposition pathway of acetaldehyde

Decomposition of acetaldehyde involves acetic acid (CH₃COOH) intermediate for decomposition to CO₂.^{7,8}



Note 6

Activity evaluation

2-propanol (IPA) decomposition was chosen to evaluate photocatalytic activity due to its clear reaction route and detectable intermediate products like acetone. Decomposition of one IPA molecule to one acetone molecule is a one photon reaction, whilst the total decomposition of one IPA molecule to three CO₂ molecules requires 18 photons.^{5,6} In this experiment, we use a photoacoustic multi-gas monitor (INNOVA AirTech Instrument A/S) to measure the concentrations of IPA, acetone, and CO₂. The specific experimental process for gas monitor analysis is outlined below,

First, 0.2 g of photocatalyst powder was dispersed in ultra-pure water, poured into a glass Petri dish, and left to dry (light exposed area = 5.5 cm²). The photocatalyst on a dish was then placed in a well-sealed 0.5 L reactor. Before each IPA decomposition test, the photocatalyst was pre-irradiated to remove any organic contamination from the photocatalyst. Pre-irradiation consists of introducing (99.9 %) pure air into the glass reactor and then shining a xenon lamp on the

photocatalyst for over 12 h. A 150 W xenon lamp (HAYASHI-REPIC, LA-410UV -3, 150 W) and a green LED (HAYASHI-REPIC, TKG-3150-2100, 80W) were used as the light sources.

One limitation of this photoacoustic multi-gas monitor is that a time interval exists before detection, this limitation makes the initially detected organic molecules concentration is slightly lower than actually injected one due to chemisorption of organic molecules onto surface of catalyst during that interval.

Note 7

Calculation of turnover number.

In the Fe(III)-BiVO₄ system, the Fe(III) nanoclusters act as the reaction site. The optimum amount of Fe(III) is 0.6 wt% and for each test 0.2 g of catalyst was used. So the amount of Fe

is calculated as $\frac{0.2 \times 0.6 \times 10^{-2}}{55.845} \times 10^6 = 21.49 \mu\text{mol}$. The total amount of CO₂ generated is obtained by summing the CO₂ generated from each of the 4 repeat tests (Fig. S6): 11.62 + 10.66 + 8.75 + 7.39 $\mu\text{mol} = 38.42 \mu\text{mol}$. Each mole of CO₂ generated through IPA decomposition requires 6 electrons and so the turnover number (TON) is calculated using the following equation:

$$TON = \frac{6 * \text{generated } CO_2 \text{ amount } (\mu\text{mol})}{Fe(III) \text{ amount } (\mu\text{mol})}$$

The turnover number of Fe(III)-BiVO₄ is found to be 10.73.

Note 8

Detail of quantum yield calculation and action spectra

The action spectra were determined by measuring the photocatalytic activity under irradiation by a monochromatic light source (BUNKOUKEIKI, BIX-300) within a tunable wavelength center at either 610 nm, 590 nm, 570 nm, 550 nm, 510 nm, 490 nm, 450 nm and a half width of 50 nm. The adsorbed photon number was calculated using the following equation:

$$N_{ads \text{ photon}}(\text{mol}) = \frac{1}{N_{A300 \text{ nm}}} \int_{300 \text{ nm}}^{800 \text{ nm}} \frac{\lambda P(\lambda) SR(\lambda)}{hc} \left(\frac{l'}{l}\right)^2 d\lambda$$

in which:

- λ refers to wavelength,
- $P(\lambda)$ refers to the spectral power density distribution of the monochromatic light source at the corresponding wavelength (which was measured by USHIO USR-45 spectroradiometer),
- S refers to the irradiation area of the photocatalyst,
- and $R(\lambda)$ represents the reflection ratio measured by UV-Vis spectroscopy.

h , c and N_A are Planck constant, light velocity, and Avogadro number respectively.

The quantum yield was calculated using the following equation, in which $n_{acetone}$ is the amount of acetone generated and $N_{ads\ photon}$ is the total number of photons generated in this period.

$$\Phi = \frac{n_{acetone}}{N_{ads\ photon}} \times 100\%$$

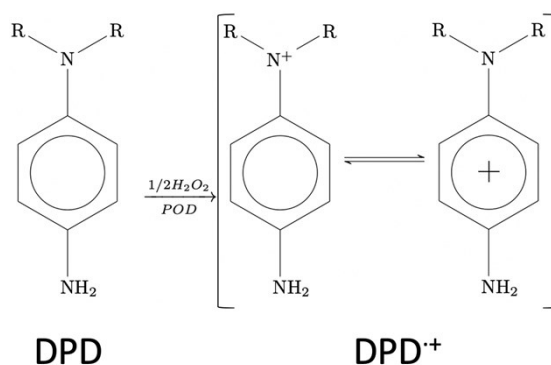
In this research, we used acetone generation for the estimation of quantum yield, as was done in a previous study.⁹ This is because the acetone generation pathway is quite simple and we do not need to consider CO₂ contamination from the ambient air. Spectra of monochromatic light sources are shown in Fig. S10.

Note 9

Detection of H₂O₂ generated by photocatalyst through DPD method.

1. Mechanism of DPD method

Detection of H₂O₂ was conducted by following a previously reported DPD method.¹⁰ Its mechanism is described below.



Peroxidase (POD) can be oxidized by H₂O₂ to a higher valence state, which in turn oxidizes DPD to radical cation denoted as DPD⁺. Detection of DPD⁺ is easy by observing its optical absorbance, since it will form stable color with absorption peaks at 510 nm and 551 nm.

2. Detailed experimental procedure for H₂O₂ detection.

50 mg pristine BiVO₄ and Fe(III)-BiVO₄ were evenly distributed onto a glass Petri dish (5.5 cm²) and then been put into sealed reactor in the same manner with the one used in activity evaluation. 3 μmol of IPA was subsequently injected, and the photocatalytic reaction was driven by Xenon lamp irradiation for 23 min.

After the photocatalysis test of IPA decomposition under visible light irradiation, powder was immediately collected and dispersed into aqueous solution containing 27 mL water, 3mL buffer (1×10⁻³ M Na₂HPO₄ and 9×10⁻³ M NaH₂PO₄ dissolved in 100 mL distilled water), 10 μL CH₃OH, 100 μL DPD solution (0.1g DPD·H₂SO₄ (Wako Co., Ltd) dissolved in 10 mL distilled water), and 100 μL POD solution (10 mg POD (Wako Co., Ltd) dissolved in 10 mL distilled water). After stirring for 5 min, suspension was centrifugated for separation of photocatalyst powder from the solution, then the absorption spectrum of upper solution was measured by an UV-Vis spectrophotometer.

Supplementary Figures

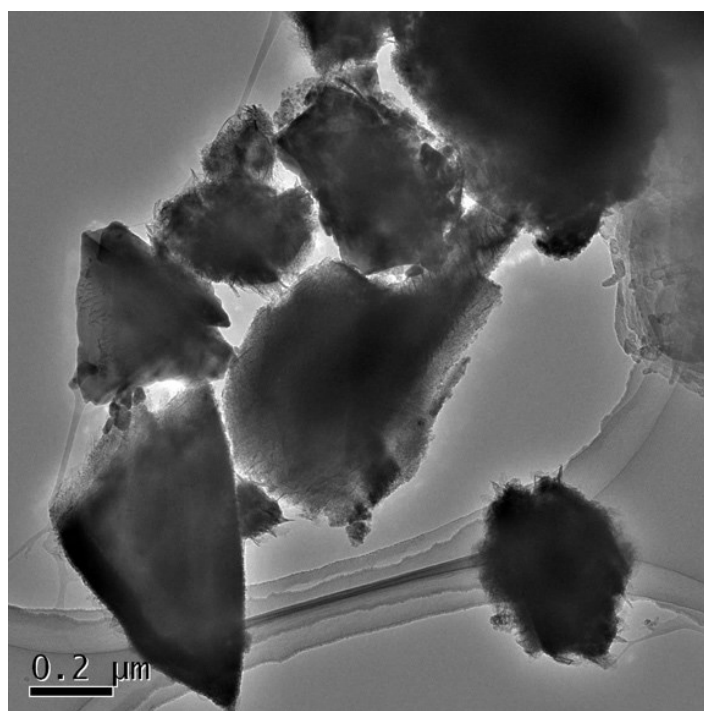


Fig. S1 TEM image of BiVO₄ synthesized through solid state reaction.

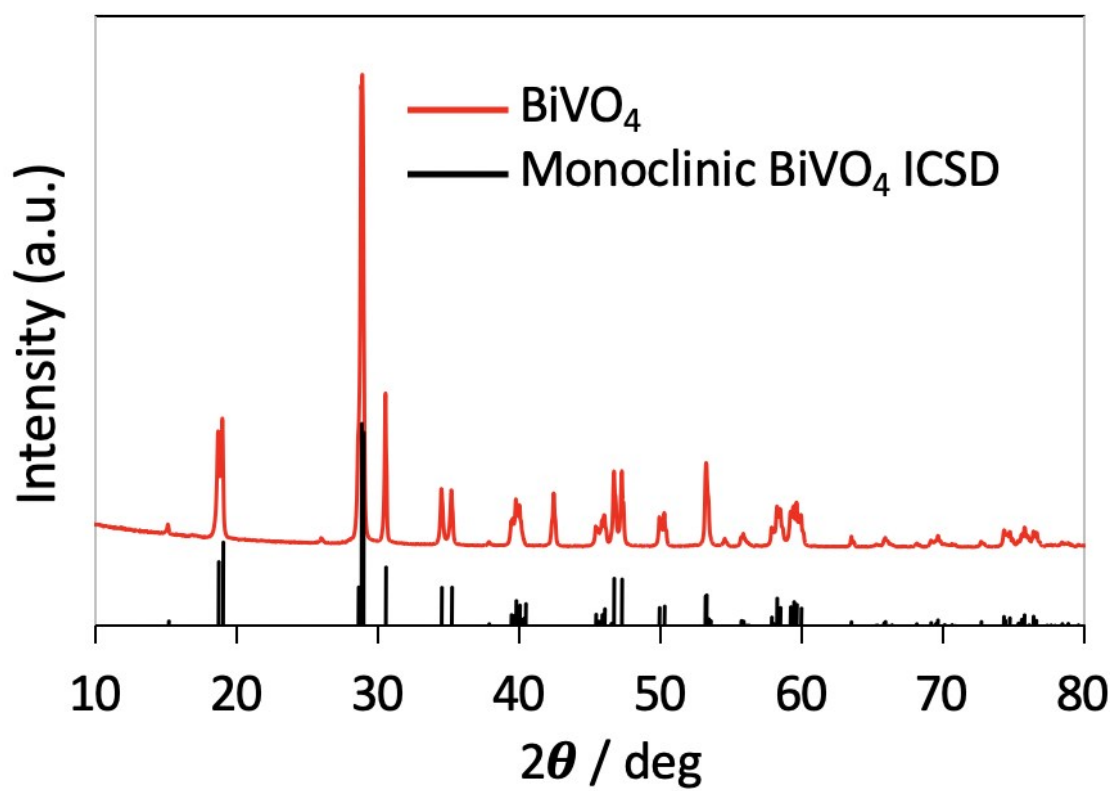


Fig. S2 XRD pattern of bare BiVO₄.

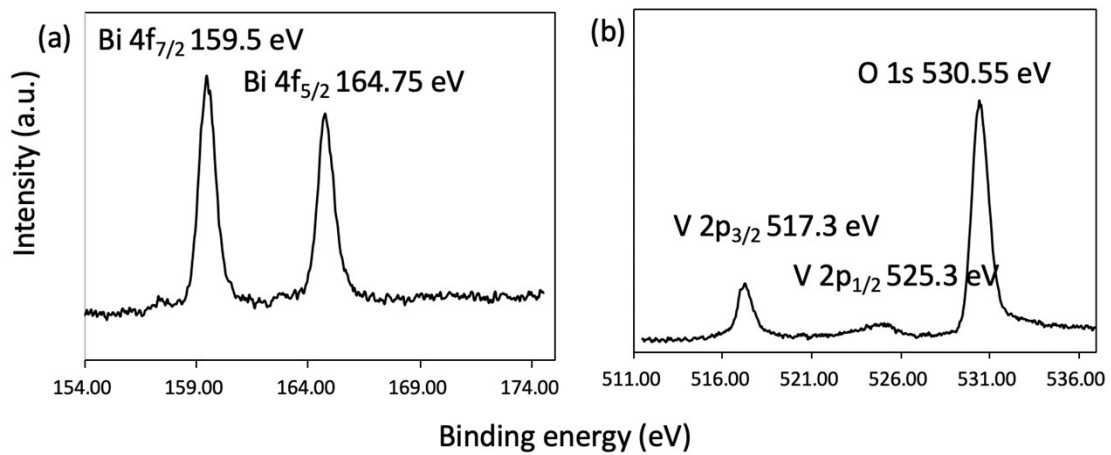


Fig. S3. HXPES spectra of Bi 4f (a) and V 2p (b).

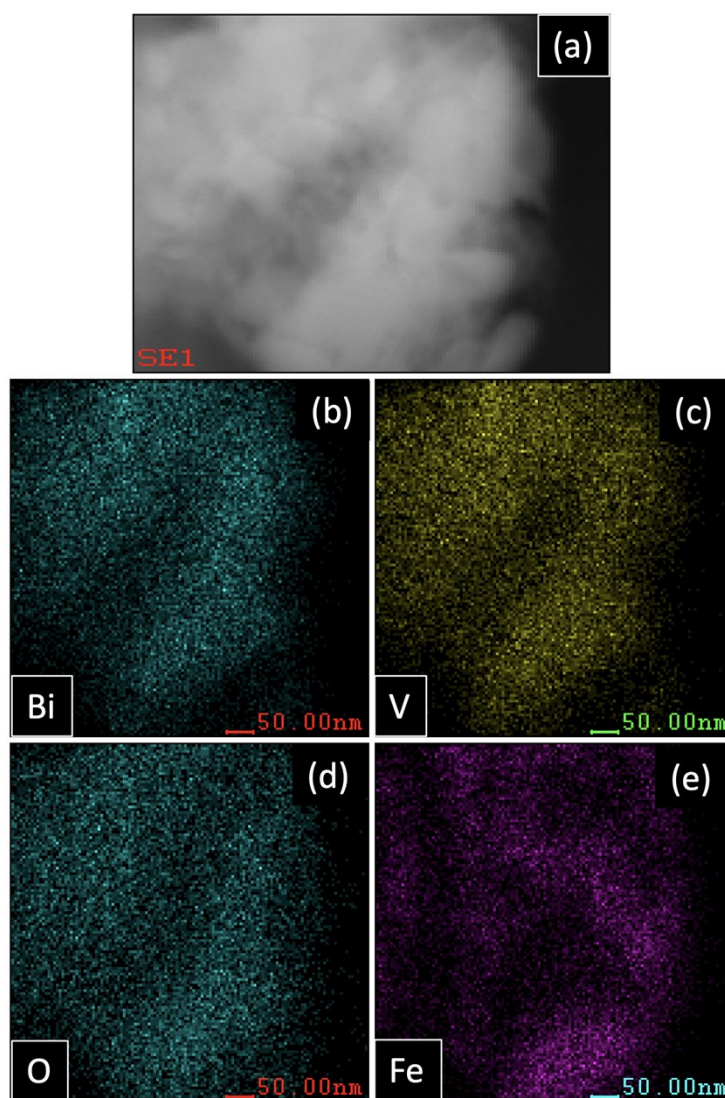


Fig. S4 STEM image of Fe(III)- BiVO₄ (a), EDS elemental mapping of Bi (b), V (c), O (d), and Fe (e), respectively.

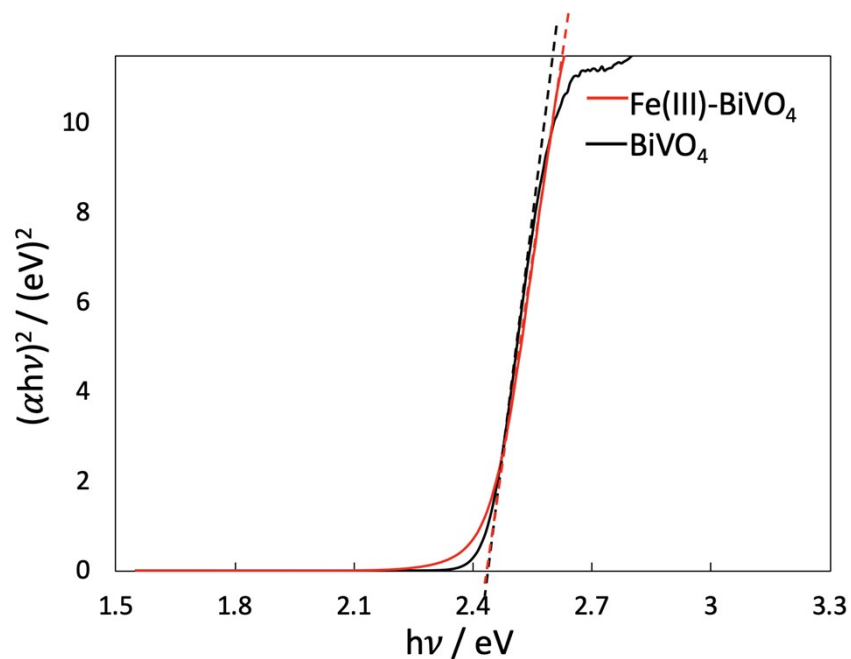


Fig. S5. Tauc plots for estimating the bandgap of BiVO_4 and Fe(III)-BiVO_4 .

Tangent line for these slopes were intercepted at the same energy value in the horizontal axis, indicating that the modified Fe(III) species did not influence the intrinsic bandgap value of BiVO_4 . On the other hand, extended absorption shoulder in low energy region was seen in Fe(III)-BiVO_4 , which would be ascribed to interfacial charge transfer other than bandgap excitation of BiVO_4 itself.

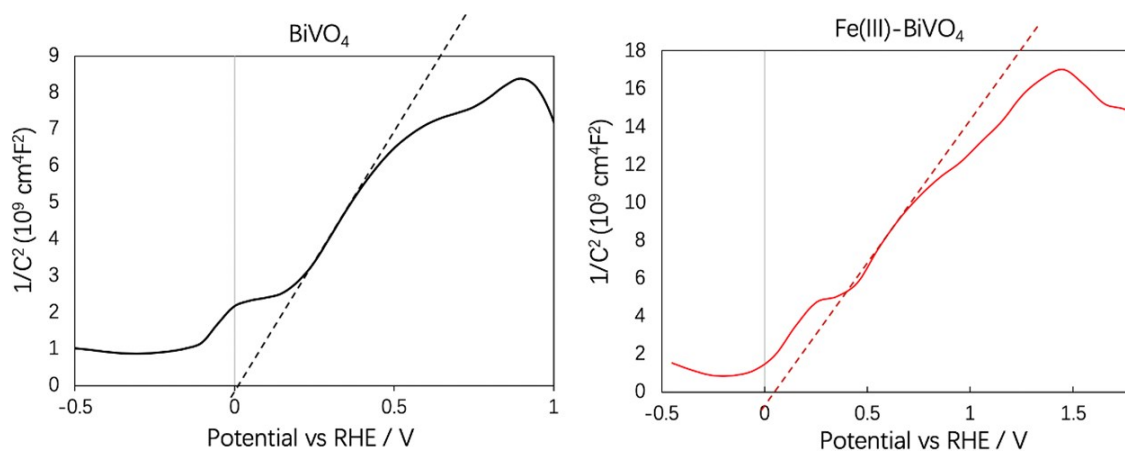


Fig. S6 Mott-Schottky plot of bare BiVO_4 and Fe(III)-BiVO_4 .

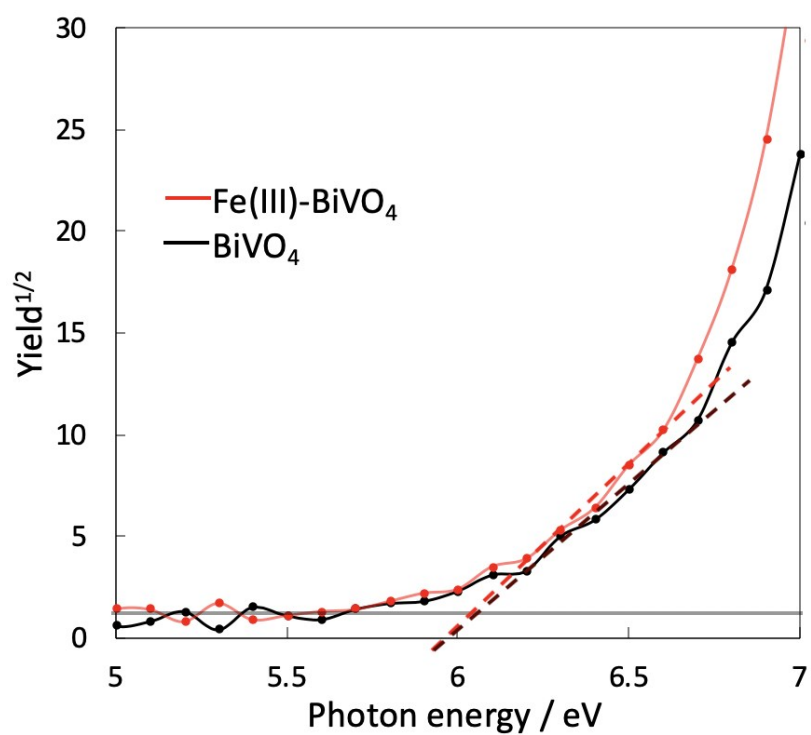


Fig. S7 Photoemission yield spectra (PYS) of pristine BiVO₄ and Fe(III)-BiVO₄.

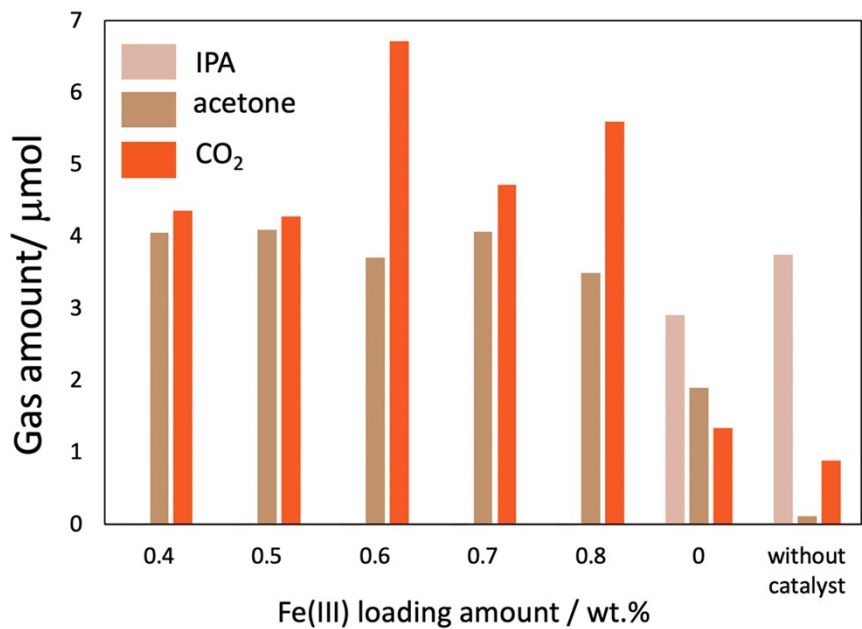


Fig. S8. Amount of acetone and CO₂ generated through IPA oxidation after 16 h under xenon lamp irradiation.

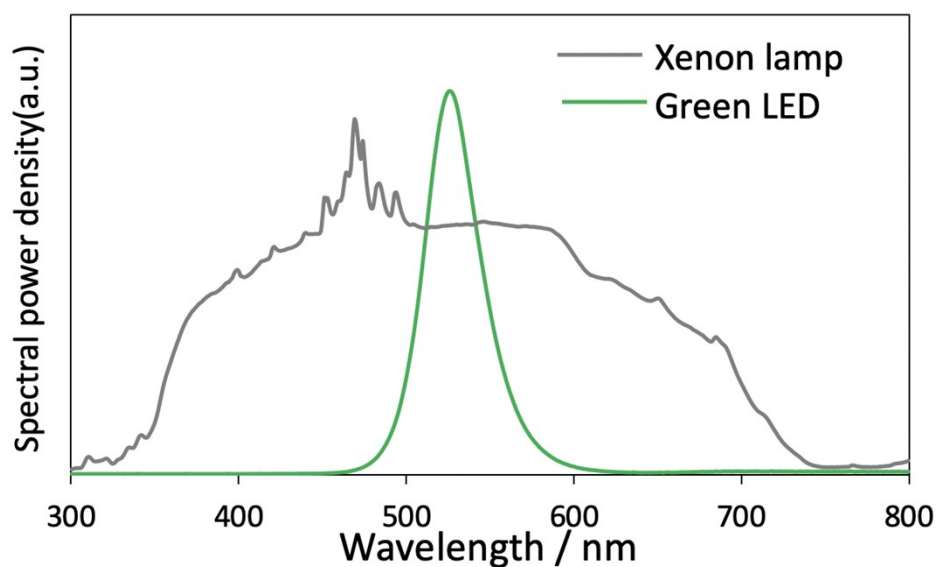


Fig. S9. Spectra of xenon lamp and green LED used

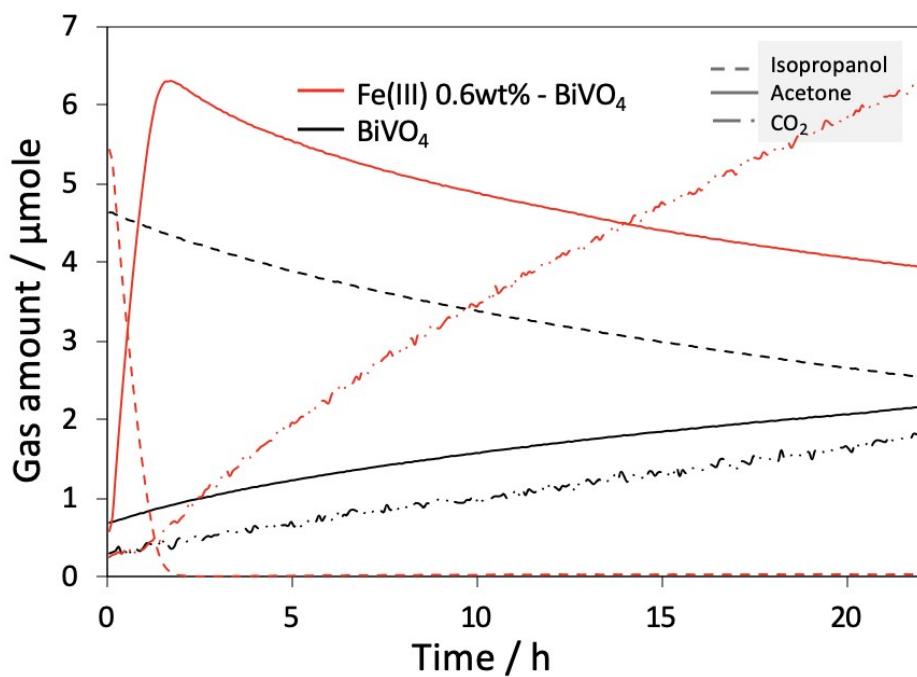


Fig. S10. IPA decomposition in the presence of pristine BiVO₄ (black lines) and optimized Fe(III)-BiVO₄ under xenon lamp irradiation (red lines). Dashed lines, solid lines, and dotted lines correspond to IPA, acetone, and carbon dioxide, respectively.

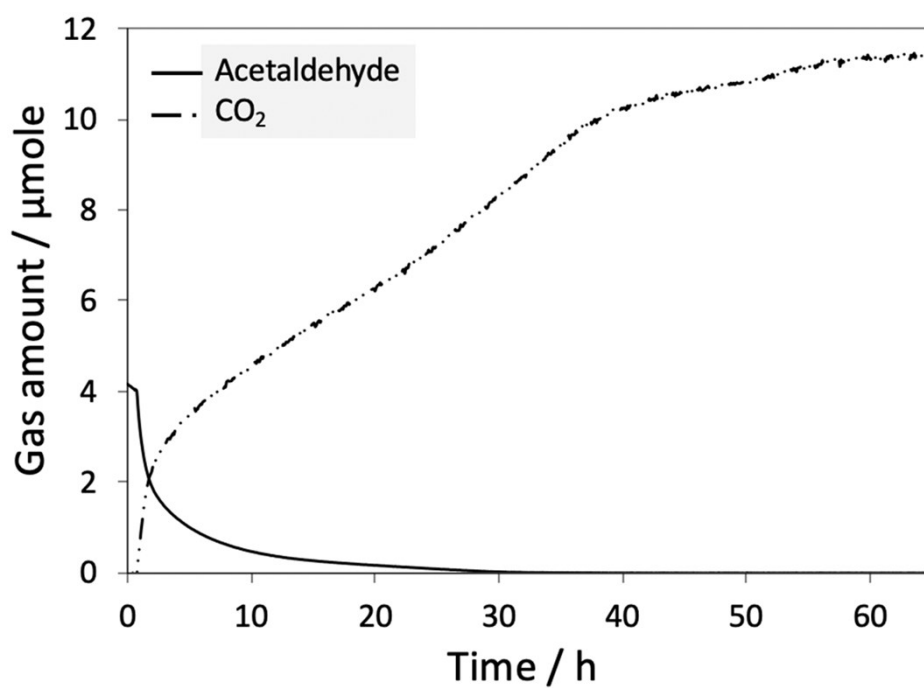


Fig. S11. Photocatalytic decomposition of acetaldehyde by Fe(III)-BiVO₄ under xenon lamp irradiation.

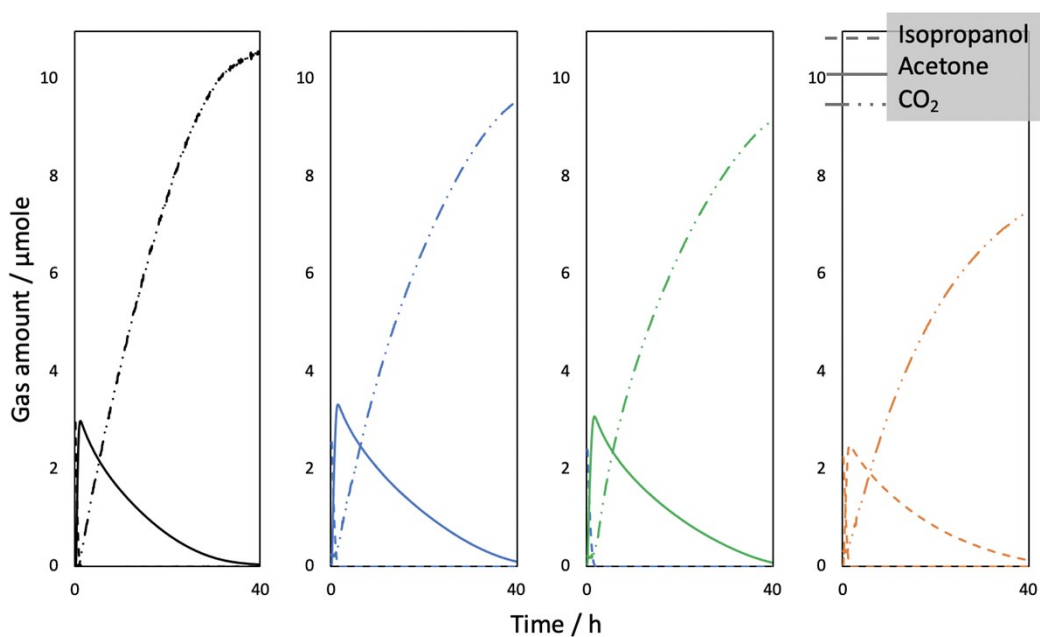


Fig. S12. Repeated test of Fe(III)-BiVO₄ for the decomposition of IPA under xenon lamp irradiation.

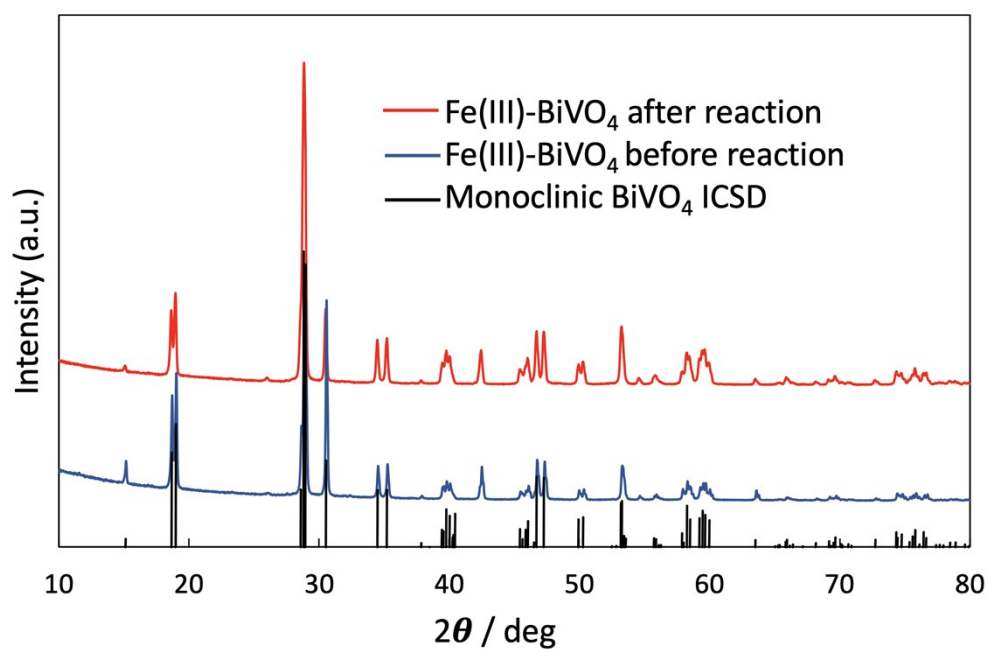


Fig. S13. XRD patterns of Fe(III)-BiVO₄ before and after photocatalysis reaction.

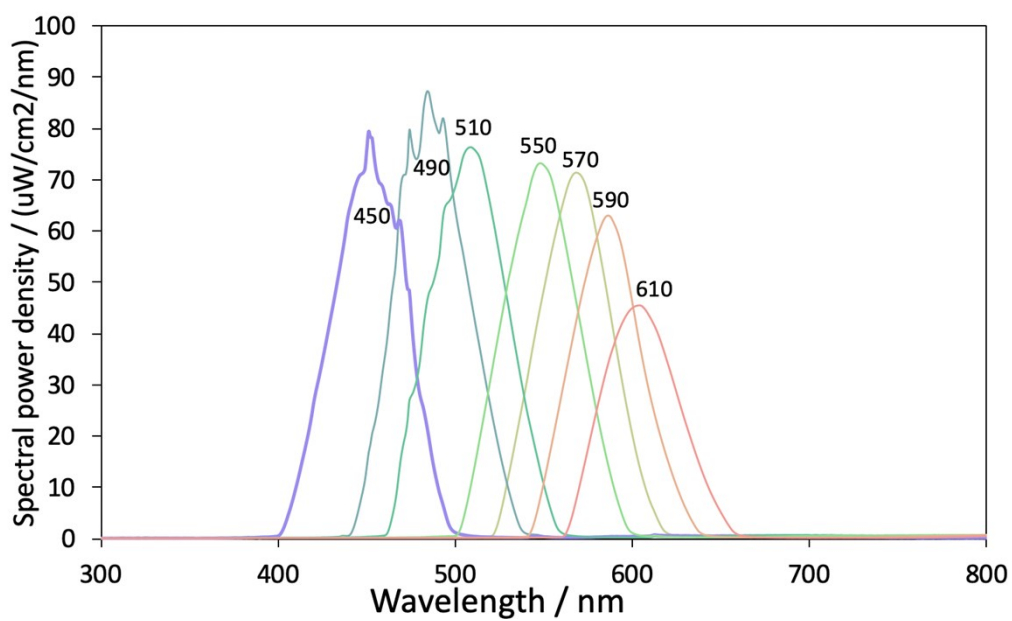


Fig. S14. Spectra of monochromatic light sources, each with the central wavelength labeled.

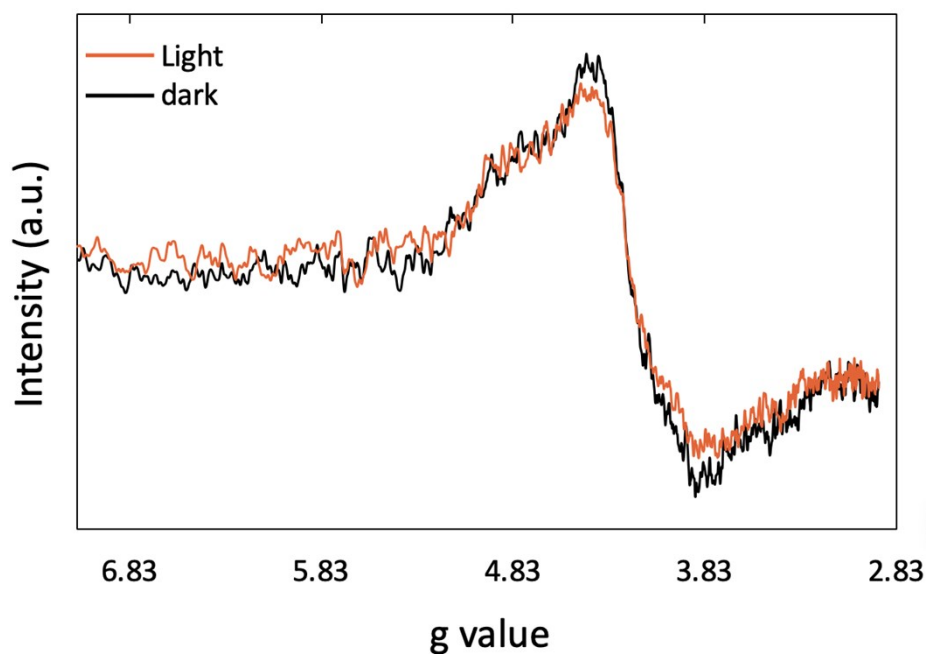


Fig. S15. ESR spectra of Fe(III)-BiVO₄ in the dark (black line) and under visible light irradiation (orange line) in a nitrogen atmosphere.

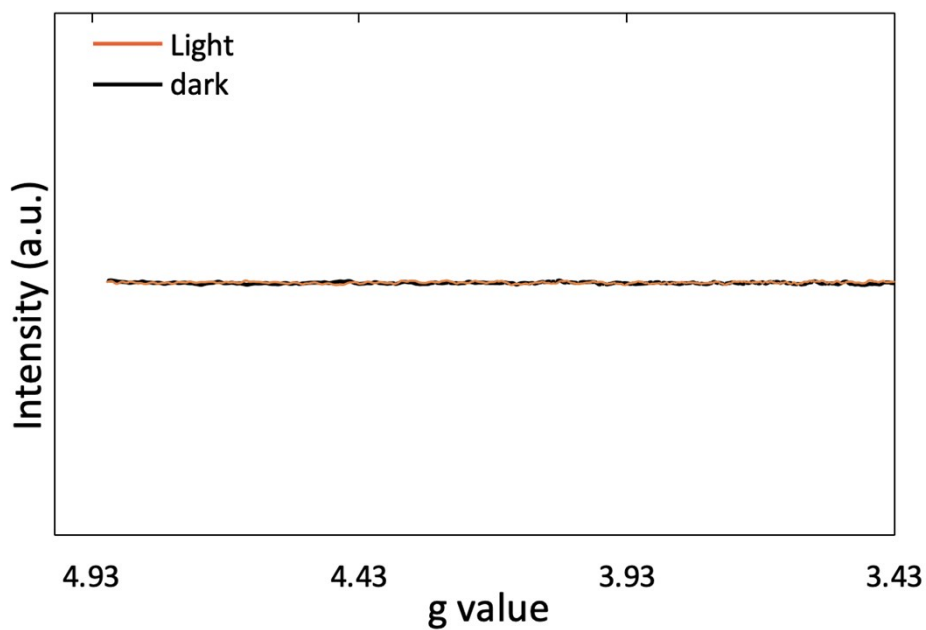


Fig. S16. ESR spectra of bare BiVO₄ in the dark (black line) and under visible light irradiation (orange line) in a nitrogen atmosphere.

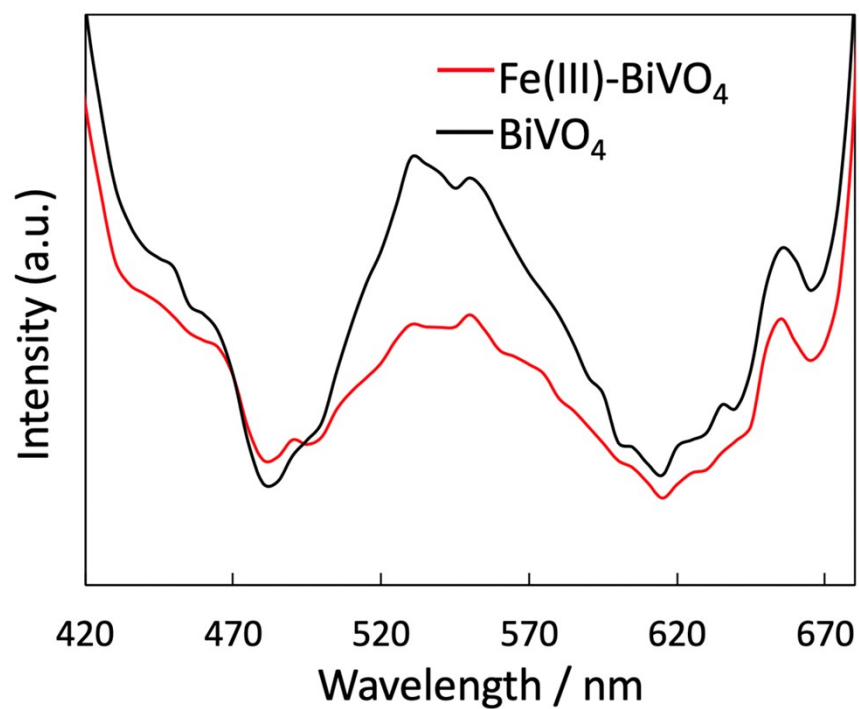


Fig. S17. PL spectra of pristine BiVO_4 and Fe(III)-BiVO_4 with an excitation wavelength at 355 nm under ambient condition.

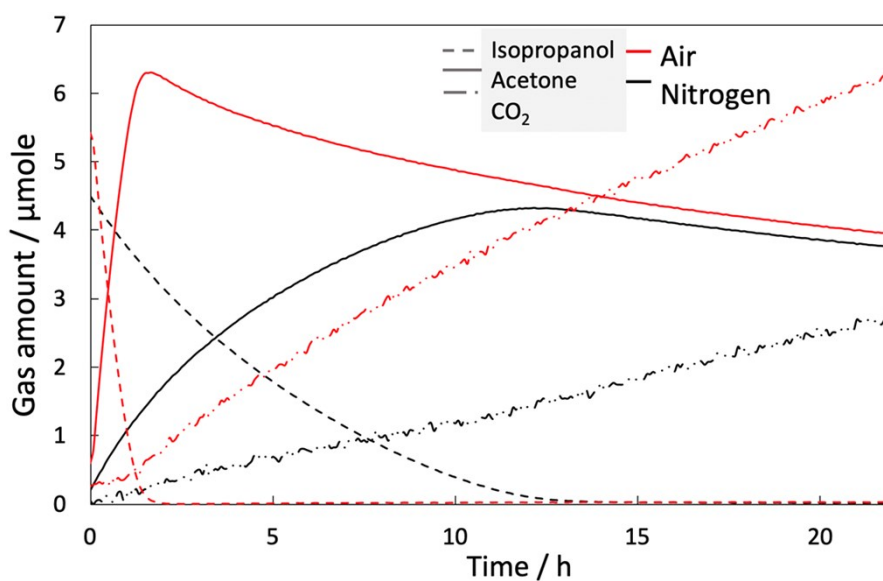


Fig. S18. Photocatalytic decomposition of IPA over Fe(III)-BiVO_4 under air atmosphere (red line) and nitrogen-rich atmosphere (black line) under visible light irradiation. In the nitrogen-rich atmosphere, we adequately flowed nitrogen gas into a glass reactor before IPA injection and light irradiation.

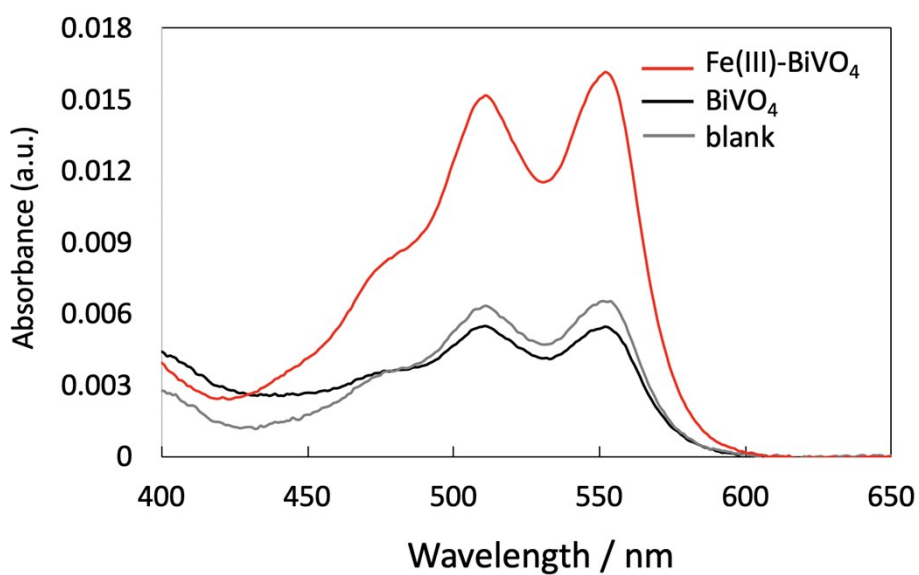


Fig. S19. Absorption spectra of upper solution of suspension (DPD/POD solution with photocatalyst powder (red: Fe(III)-BiVO₄, black: BiVO₄), which undergoes a photocatalytic IPA decomposition for 23 min), and a blank result without catalyst addition (gray line). Peaks at 510 nm and 551 nm are assigned to the formation of H₂O₂.

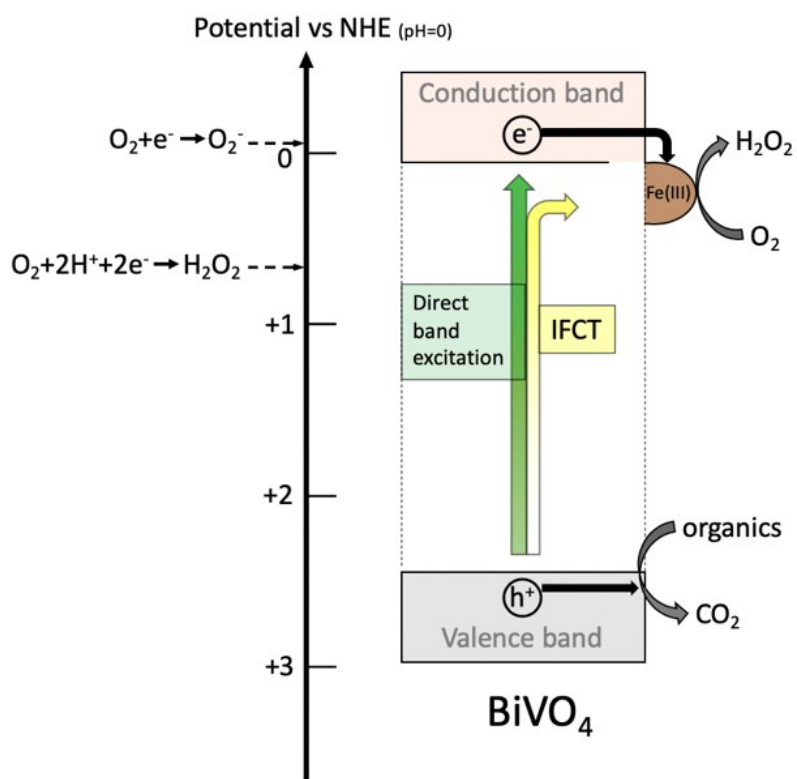


Fig. S20. Reaction scheme of Fe(III)-BiVO₄ for organic decomposition.

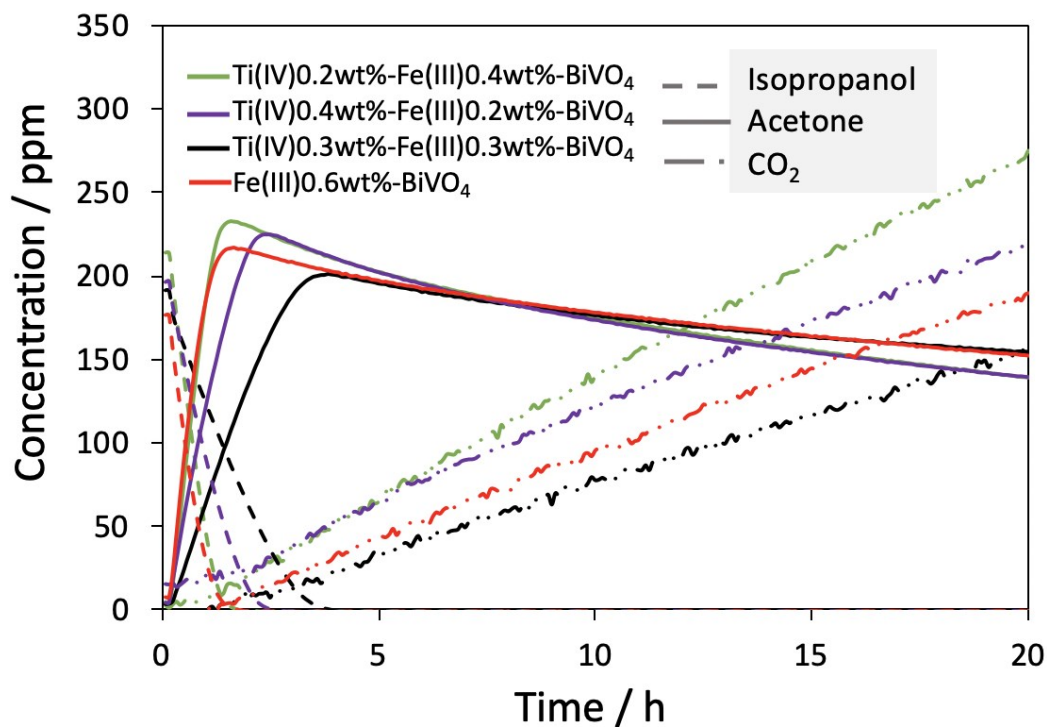


Fig. S21. IPA decomposition in the presence of Ti(IV) and Fe(III) cluster co-modified BiVO₄ under xenon light irradiation.

According to previous studies^[1,2], Ti(IV) nanoclusters act as a promoter for oxidation activity. The present results are consistent with these previous studies, *i.e.* the rate of CO₂ generation is faster in the presence of BiVO₄ co-grafted with Ti(IV) and Fe(III) nanoclusters than in the presence of BiVO₄ grafted only with Fe(III) nanoclusters.

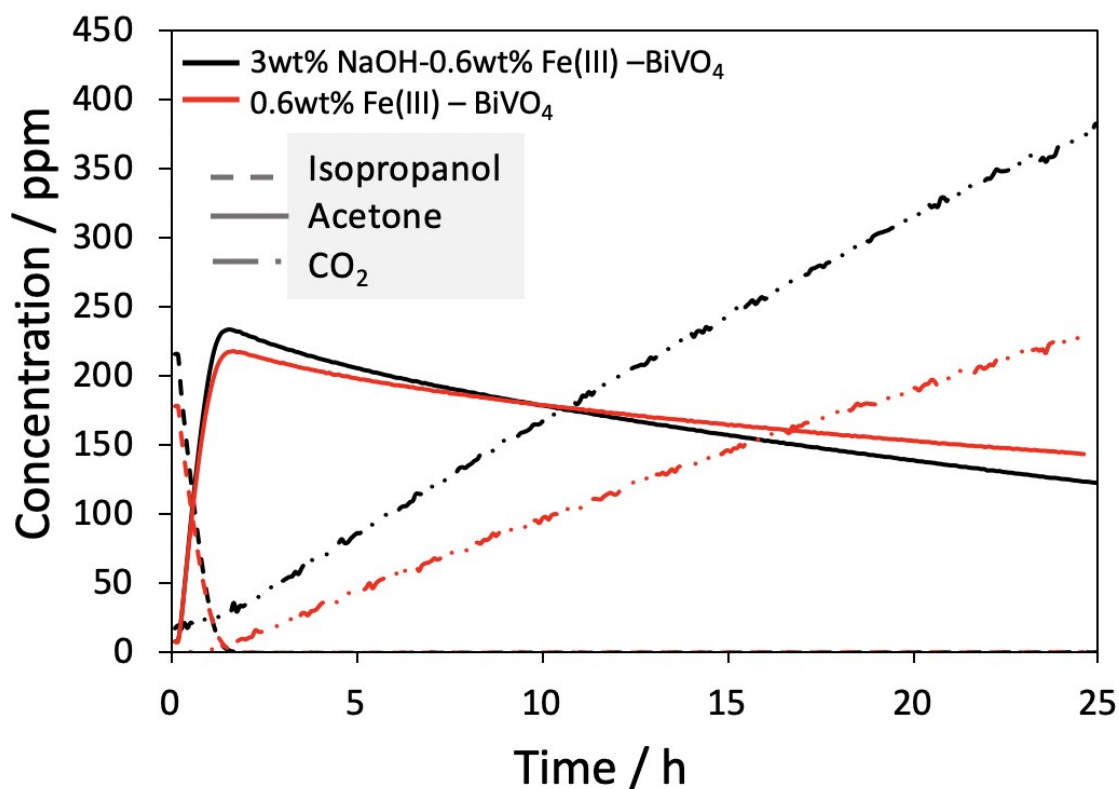


Fig. S22. Comparison of IPA decomposition in the presence of Fe(III) modified, alkaline treated BiVO₄ with IPA decomposition the presence of Fe(III) modified, non-alkaline treated BiVO₄.

Surface contamination inhibits charge transfer at the interface. Alkaline treatment removes surface contamination on BiVO₄ and so improves the visible light activity of Fe(III)-BiVO₄.

References,

- 1 R. Inde, M. Liu, D. Atarashi, E. Sakai and M. Miyauchi, *J. Mater. Chem. A*, 2016, **4**, 1784–1791.
- 2 M. Liu, R. Inde, M. Nishikawa, X. Qiu, D. Atarashi, E. Sakai, Y. Nosaka, K. Hashimoto and M. Miyauchi, *ACS Nano*, 2014, **8**, 7229-7238.
- 3 T. Kako, X. Meng and J. Ye, *Appl. Catal., A*, 2014, **488**, 183-188.
- 4 S. J. Hong, S. Lee, J. S. Jang and J. S. Lee, *Energy Environ. Sci.*, 2011, **4**, 1781–1787.
- 5 F. Arzac, D. Bianchi, J. Chovelon, C. Ferronato and J. Herrmann. *J. Phys. Chem. A*, 2006, **110**, 4202-4212.
- 6 F. Arzac, D. Bianchi, J. Chovelon, C. Ferronato and J. Herrmann. *J. Phys. Chem. A*, 2006, **110**, 4213-4222.
- 7 M. R. Nimlos, E.J. Wolfrum, M. L. Brewer, J. A. Fennell and G. Bintner, *Environ. Sci. Technol.*, 1996, **30**, 3102-3110
- 8 D. S. Muqqli, J. T. McCue and J. L. Falconer, *J. Catal.*, 1998, **173**, 470-483.
- 9 Y. Ohko, K. Hashimoto and A. Fujishima, *J. Phys. Chem. A*, 1997, **101**, 8057-8062.
- 10 H. Bader, V. Sturzenegger and J. Hoigne, *Water Research*, 1988, **22**, 1109-1115.